Cast in Steel 2021
Designing, Modeling, Casting, and Testing of Thor's Hammer:
Mjölnir "The Giant Killer"

Team Members:
Corinne Wells
Manuel Umanzor
Tristan Pagkalinawan

Faculty Advisor:
Dr. Alan P. Druschitz

Virginia Tech, Department of Materials Science and Engineering &
Virginia Tech Foundry Institute for Research and Education

Foundry Partner: D.W. Clark

Special Thanks: Southwest Specialty Heat Treat & ExOne

Abstract:

For our submission we based our design off of the Marvel version of Thor's hammer. Our goal was to produce the largest hammer within the parameters. After several iterations we settled on a hollow design with columns that support the point of largest deflection point determined using FEM. Lettering along the sides the highlight our foundry, VT-FIRE, and our foundry partner D.W. Clark. Our foundry partner made our molds using 3D binder jetting technology and our cores were made by ExOne. We evaluated several alloys and, based on our hardness and toughness needs, we selected 8640 steel as our cast alloy. We melted our steel alloy and poured our casting at the foundry on campus. We had issues with the cores and lettering inserts shifting and filling the thin lattice sections along the sides of the casting. Southwest Specialty Heat Treat first normalized our casting and then austenitized, quenched and tempered our casting. A fiberglass tube was used as the handle that was then finished with brown paracord wrapping. We determined that our hammer's microstructure was tempered martensite with a hardness of 52 HRC. Our final hammer weighed 5.7 lbs and it bears a strong resemblance to the Marvel design.

***Introduction*:**

Although there were many ancient gods of Norse mythology that people prayed to, Thor was considered the “god of the people” [1]. His strength and steadfastness in his sense of justice brought many followers, most notably the Vikings. Gifted to him by his father Odin, Thor has wielded his hammer Mjölnir to slay many of his foes. The silhouette of Thor’s hammer, Mjölnir, is deeply attached to its representation of strength and power. Many followers wore pendants that represented the god of thunder and they varied widely in detail depending on the wearer's status, Figure 1 [2]. In many older illustrations, his hammer is modeled after modest striking tools. It was not until the current Marvel franchise that we see the oversized large square hammer design, Figure 2. This hammer draws inspiration on the stock silhouette of the Norse representation of Mjölnir [1]. Based on the fact that almost all of Thor’s poems and stories are about him killing giants we thought he should have a hammer that represents that [1]. For this giant killing reason, we based our design on the Marvel version as we wanted to create the largest hammerhead possible.

Figure 1. Variations in Mjolnirs pendant design through the ages and the hammer design used in the Marvel movie franchise [2], [3].

Figure 2. Replica of the prop Mjölnir used in the Marvel movies [4].

Design:

Our initial design was created in proportion to a 3D drawing of the Marvel Mjölnir prop found online [5], several modifications were made to meet the competition requirements. Starting from a hollow shell, a total of four designs were analyzed. Symmetric boundary conditions were applied to effectively model 1/8 of the hammer head, this helped reduce computational cost and saved time in turn. Figure 3 shows 1/8 cut outs of the hammer designs.

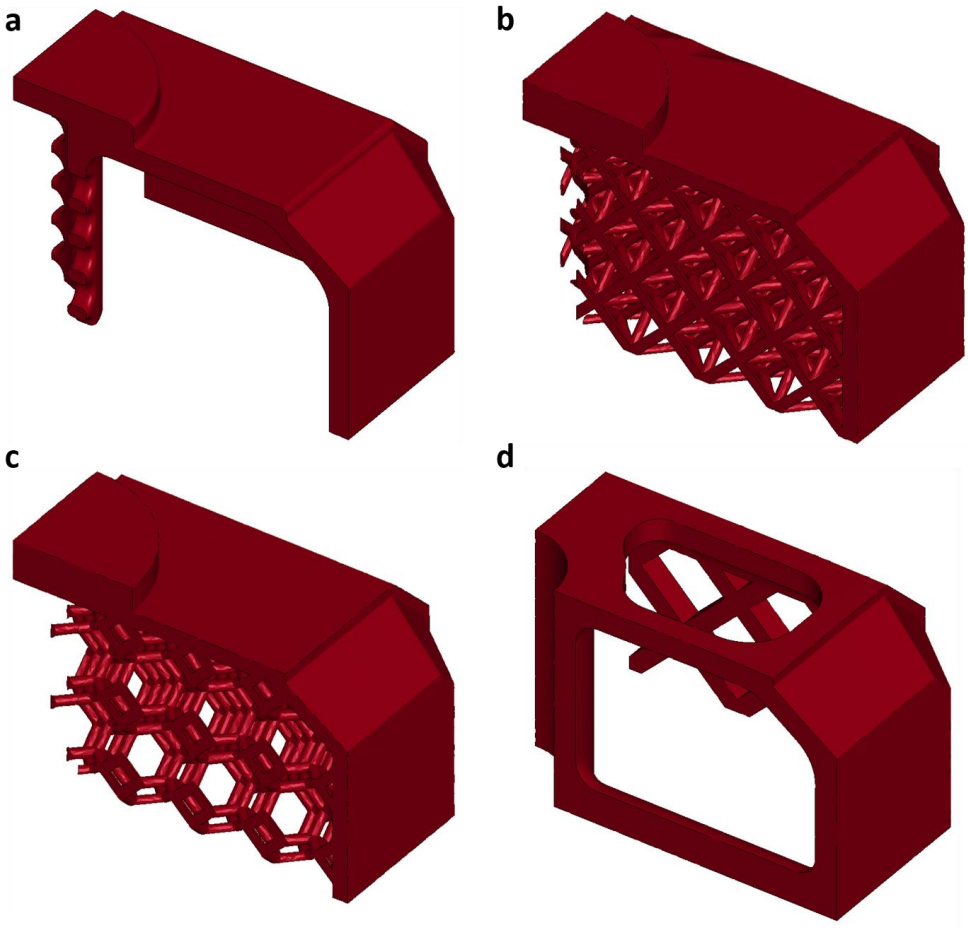

Figure 3. Design alternatives: (a) hollow shell, (b) hollow shell with octet lattice infill, (c) hollow shell with Kelvin's cell lattice infill and (d) final design.

In addition to the symmetric boundary conditions described above, a fixed constraint was applied on the internal surfaces of the hole in which the handle would be installed later, and a prescribed motion load was applied on the striking face as shown in Figure 4. Given the weight limit of (≤ 6 lb), each design was scaled such that every instance would be compliant with the weight, Table 1 lists the resulting different truss diameters and dimensions.

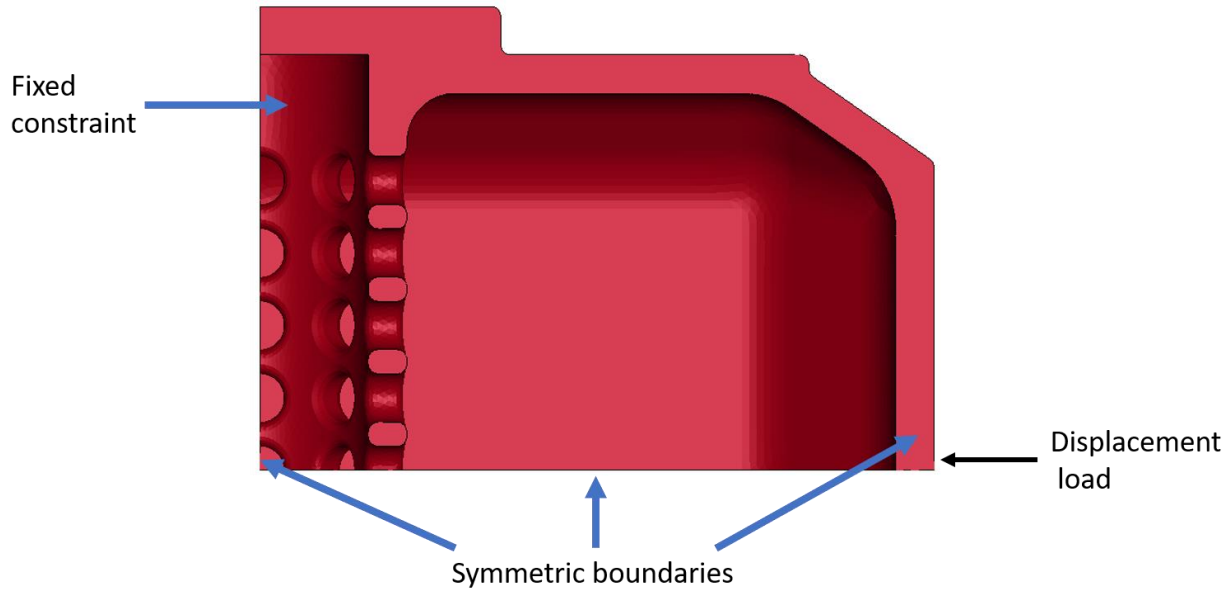

Figure 4. Loading and boundary conditions.

Table 1. Design iterations with their estimated weights.

Design	Infill	Weight (lb)	Truss Diameter (in)	LxWxH (in)
1	Hollow	5.21	N/A	6.2x3.8x3.8
2	Octet lattice	5.49	0.079	5.5x3.3x3.3
3	Kelvin lattice	5.73	0.079	5.7x3.6x3.6
4	**Single column**	**5.49**	**N/A**	**6.3x3.9x3.9**

FEM Analysis:

The analysis of deformations was performed with the commercial package LS-Dyna®, and as starting point the material behavior was modeled using the properties of 4340 steel under the Johnson-Cook constitutive relationship [6], which expresses the flow stress as follows:

$$\sigma_y = \left(A + B\underline{\varepsilon}_p^n\right)\left(1 + C\ ln\ ln\ \dot{\varepsilon}^*\right)\left(1 - T^{*^m}\right)$$

Where, *A*, *B*, *C*, *n*, and *m* are input constants, $\underline{\varepsilon}_p$ represents the effective plastic strain, the normalized strain-rate is given by $\dot{\varepsilon}^*$ and the homologous temperature is represented by T^*. For simplicity, the temperature dependent term was neglected by selecting a simplified version of the model [7]. The specific-internal energy results of the

FE simulation indicate that the model infilled with the octet lattice structure has superior performance, Figure 5, however, from a metalcasting standpoint it is very unlikely to fill a mold with such small features (0.079 in truss diameter). The latter statement is also valid for the model infilled with the Kelvin's cell arrangement; hence, it was decided to pursue a hollow design.

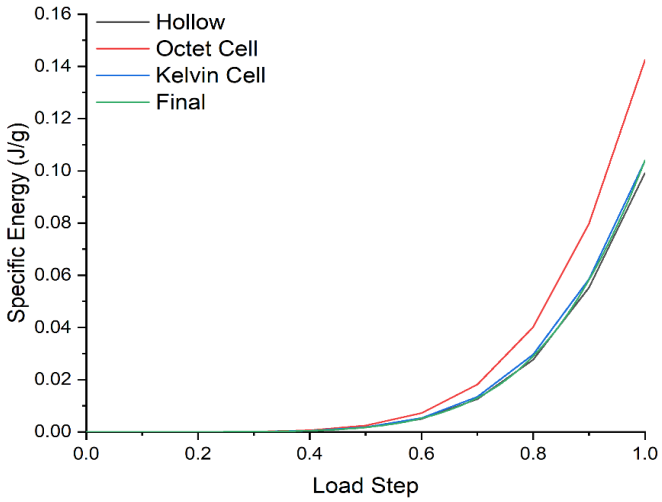

Figure 5. Specific-internal energy result from FEM

For the final design, the shell was created in such a way that its wall thickness was approximately 0.2 in, further weight reduction was achieved by creating openings on all non-striking faces and the cap on the original design was omitted. Removal of material was supported by the FEA results for von Mises stress, in which it was ascertained that these sections of the hammer have relatively low stresses, Figure 6. A CAD view of the final design is provided in Figure 7 and a technical drawing can be seen in Figure 8. The final lettering details were added later.

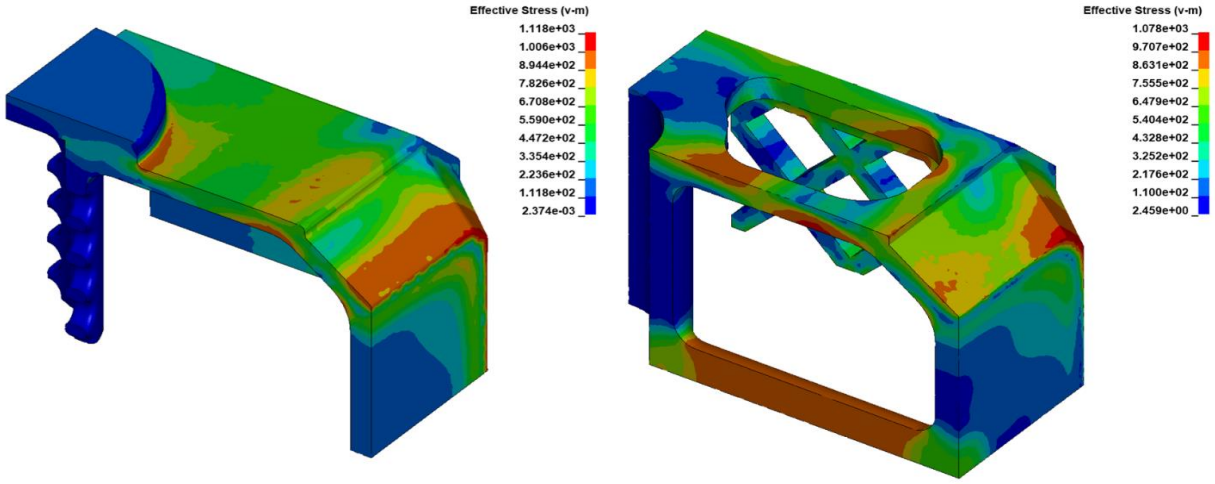

Figure 6. Fringe plots of the von Mises stresses.

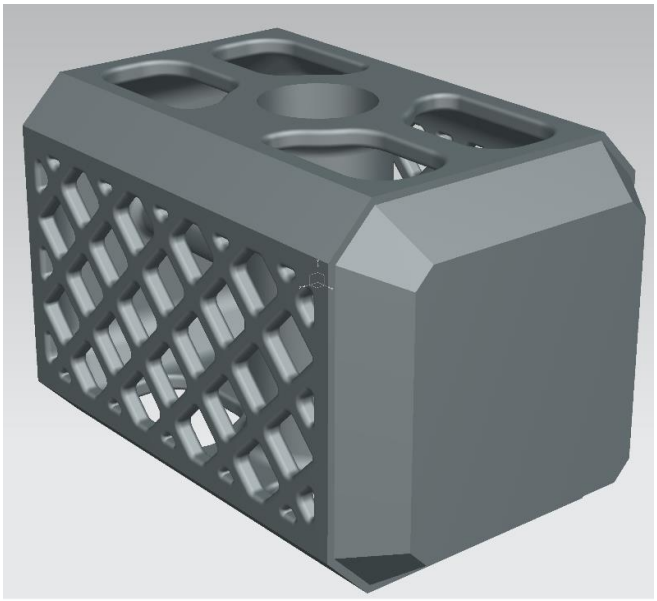

Figure 7. CAD image of final design without lettering.

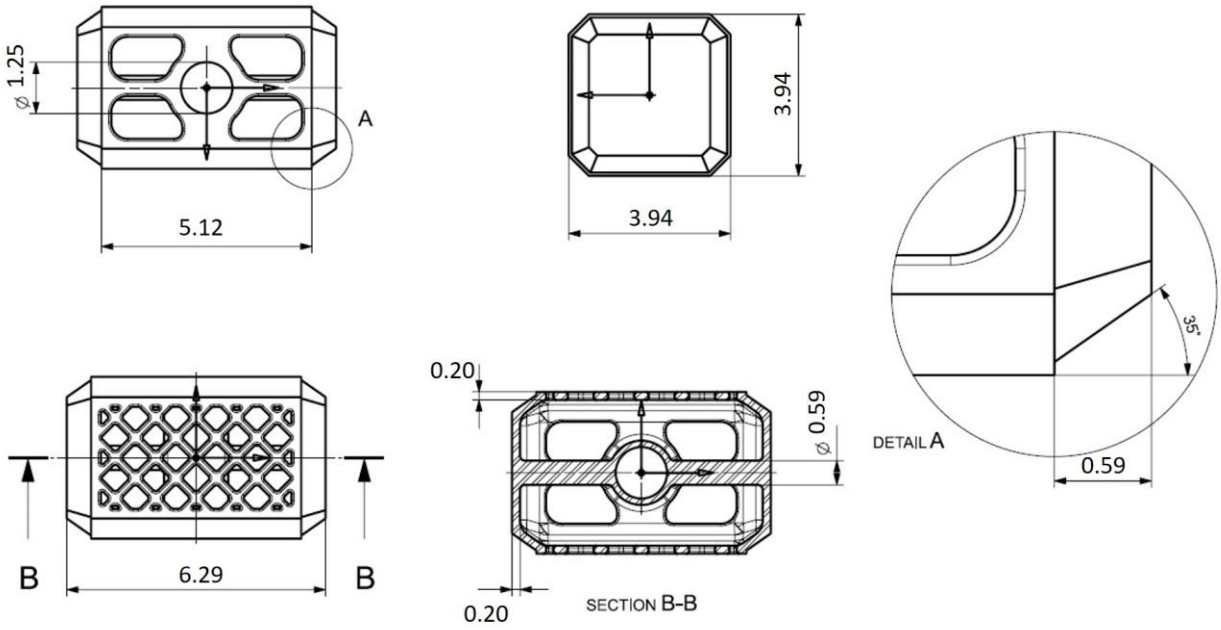

Figure 8. Technical drawing of final design. Detail A shows extrusion of striking faces and internal detailing is provided by section B-B.

Filling and Solidification Analysis:

To further support our design decision that we would have issues with pouring the other designs discussed we ran a filling and solidification modeling software, MAGMAsoft [8]. The gatling was a simple downspure straight into the mold cavity along with vents around the cavity. The modeling was used to predict issues we would have

with filling, porosity, shrinkage, and other casting related issues. The software does not have data for the alloy we wanted so we calculated thermal data using ThermoCalc [7]. Using this ThermoCalc data, we were able to input the thermal data and run a model with our alloy using the tools Furan mold database. This process of calculating and importing data into MAGMA has proven accurate as our solidus and liquidus values in the software are within 1%of our own thermal analysis data of the metal we actually poured. Figure 9 shows the MAGMA filling results using our final design and shows the temperature at the end of filling. The darker red portions show a colder metal along the lattice and on the upper portion. For this reason, we suspected we would have issues with porosity, shrinkage, and incomplete filling in those areas. For this reason, our team focused on selecting an alloy with the best chance of filling that section. The next section of this report will discuss this selection process in more detail.

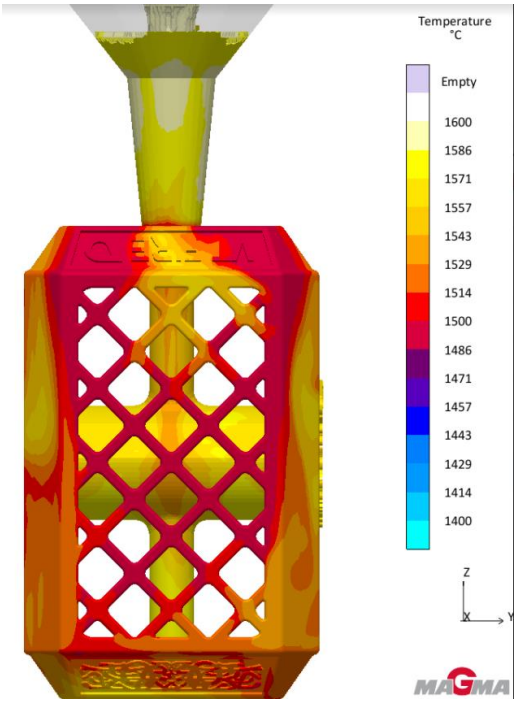

Figure 9. The temperature after filling was completed in the MAGMA model.

Cast Alloy Selection:

Our criteria for selecting an alloy were that it needed to be castable, have medium hardenability with good toughness, with low cost. Firstly, the hammer design is almost entirely thin walled so castability was extremely important. For this reason, we looked at the three low-alloy castable steels 41xx, 43xx, and 86xx [9]. The 41xx series is a Cr-Mo steel and the 43xx and 86xx steels are Ni-Cr-Mo steels.

Secondly, our team aimed to have a carbon content of 0.40 wt% as at it has a HRC range of 42.4 at 50% M to 56.1 at 99% M when quenched [10]. Companies that produce heavy striking tools temper their hammers anywhere from 45 to 55 HRC

depending on the application of that tool [11]. For our purposes, we wanted to make sure that when the hammer was used it was hard enough to prevent damage to the hammer face, while still maintaining some impact toughness. Impact toughness is important for our design so that the supporting truss can absorb the force applied to it during testing.

Our team felt that 0.40 wt% carbon would provide the flexibility to achieve a high hardness while still maintaining adequate toughness. Based on the carbon content we narrowed down the alloy selection to three choices 4140, 4340, and 8640 steels. The ASM chemistry standards for these steels are listed in Table 2.

Table 2. Lists the chemistry of the three alloys considered in wt% [9].

Alloy	**C**	**Mn**	**P**	**S**	**Si**	**Ni**	**Cr**	**Mo**
4140	0.38-0.43	0.75-1.00	0.035 max	0.040 max	0.15-0.35	-----	0.80-1.10	0.15-0.25
4340	0.38-0.43	0.60-0.80	0.035 max	0.040 max	0.15-0.35	1.65-2.00	0.40-0.60	0.20-0.30
8640	0.38-0.43	0.75-1.00	0.035 max	0.040 max	0.15-0.35	0.40-0.70	0.40-0.60	0.15-0.25

Out of these three steels, we focused on the Ni-Cr-Mo options as they have better impact strength due to the Ni-Cr interaction [8]. From there, we looked at their liquidus and solidus temperatures derived from ThermoCalc to determine if 4340 or 8640 had better castability. According to Table 3, while all the liquidus and solidus temperatures were relatively similar, 8640 has a slightly lower melting point [12]. Finally, the 8640 was cheaper to alloy as it had less expensive molybdenum and nickel compared to 4340 and higher low-cost manganese content. Due to good castability, good mechanical properties, and relatively low cost our team chose 8640 as our cast alloy.

Table 3. The liquidus and solidus temperatures for the three alloys [12].

Alloy	**Liquidus (ºF)**	**Solidus (ºF)**
4140	2,722	2,620
4340	2,724	2,622
8640	2,715	2,611

Mold Preparation:

Both the mold and the cores were additively manufactured using 3D binder jetting [13]. This process involves depositing a layer of material, typically silica sand, and then a printhead selectively deposits a binder and premixed catalyst, Figure 10 [13]. This process of layering sand and binder is repeated until the mold or core is completed. D.W. Clark printed the molds halves on their Viridis 3D printer, Figure 11. While the Viridis printer is faster, the ExOne printer can hold tighter dimensional tolerances, so ExOne was used to print the three piece core assembly and the lettering inserts. Both printers used silica sand and a Furan binder [14], [15]. The loose sand in the mold and core pieces were cleaned off with brushes and dry compressed air before they were assembled.

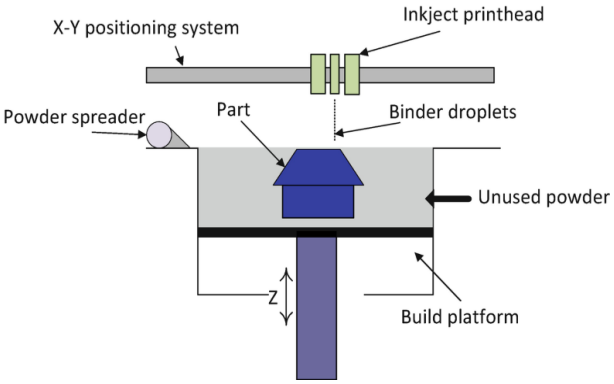

Figure 10. A schematic of the set up for binder jetting [13].

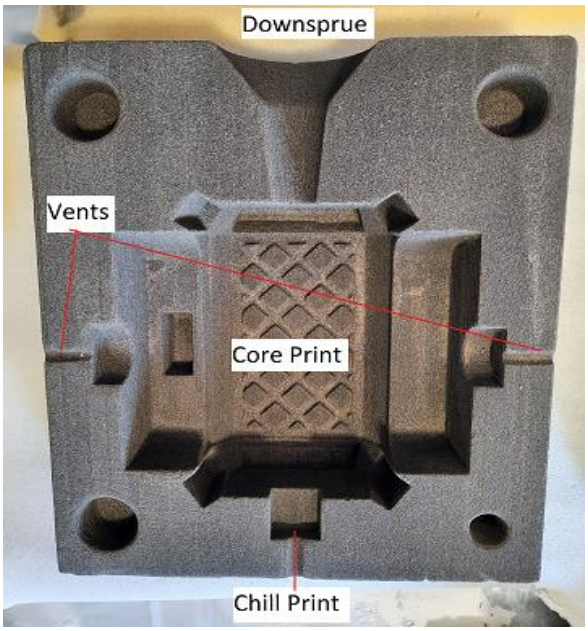

Figure 11. One half of the mold with the gating and core prints made on the Veridis printer.

A Dietert core hardness tester was used to measure the scratch hardness of the mold and the cores in order to ensure both met quality standards. The Viridis molds had an average scratch hardness of 47 while the ExOne cores were slightly harder at 52 scratch hardness. Because the walls were thin in the final design it was very important that both the mold and cores had a relatively high and consistent hardness so as to maintain dimensional tolerances during casting.

The lettering inserts were pinned into place with small nails and core paste. A circular graphite chill was placed at the bottom of the mold. This was added to make sure that there was no porosity at the striking face. The hammer cores were placed around the handle core and then placed into the mold, Figure 12. The mold was left overnight on a flat surface with weights before being clamped together and placed in a sand cart to pour.

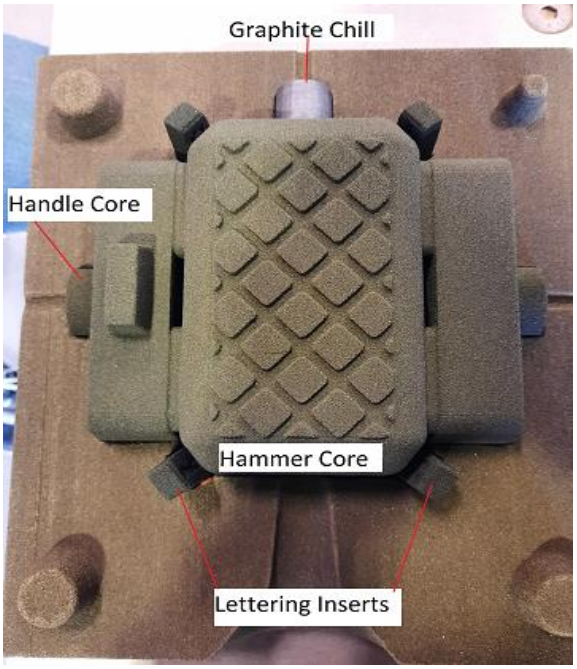

Figure 12. The core, lettering inserts, and chill assembled in the mold.

Melting and Casting:

The 8640 steel was prepared at Virginia Tech in a Inductotherm 300 lb capacity induction tilt furnace. The furnace was charged with 100 lbs of plain carbon 1045 steel. Once the charge material was molten, the silicon and manganese formed a liquid slag that was removed with a skim bar. The carbon started to react with oxygen in solution and produced a carbon boil. Once the reaction began to slow down, aluminum shot was added to the melt to kill the steel and stop the carbon boil process. Based on prior experience the chemical composition of the melt would be approximately 0.014 wt% Si, 0.055 wt% Mn, and 0.055 wt% C. The thermally stable alloying elements Cr and Ni were added to the melt at this time. Next, Sorelmetal$^{(R)}$ was added to the melt to

introduce carbon as it maximized recovery and minimized sulfur pickup. Once all the alloying elements and Sorelmetal(R) had melted, a chemistry sample was taken and the temperature was raised to 3,060ºF. Right before the furnace was tapped, 75% FeSi and 80% FeMn were added. Two grams of aluminum shot was added to the hand ladle used to pour the mold in order to ensure the steel was fully killed before going into the mold, Figure 13.

Figure 13. The handle ladle had two grams of aluminum added before it was used to hand pour the mold.

A thermal analysis and chemistry sample were hand poured before the remaining metal was pigged out. Our foundry partner, D.W. Clark used an OES spectrometer to determine the chemistry of the cast material. Table 4 shows the charge calculation target, the final chemistry of the casting, and specification for 8640. Figure 14, located in the appendix, contains the charge calculations.

Table 4. Lists the target, final and standard chemistries for the selected alloy in wt% [9].

	C	**Mn**	**P**	**S**	**Si**	**Ni**	**Cr**	**Mo**	**Al**
Target	0.44	0.90	-----	-----	0.40	0.65	0.55	0.20	0.03
Final	0.43	0.83	0.017	0.006	0.41	0.67	0.46	0.20	0.02
8640 [8]	0.38-0.43	0.75-1.00	0.035 max	0.040 max	0.15-0.35	0.40-0.70	0.40-0.60	0.15-0.25	-

Degating and Grinding:

The mold was broken open after 1 hour and allowed to cool in air overnight, Figure 15. A hand saw was used to cut off the downsprue, vents, and flash. The striking faces, sides, and lettering were hand ground with a pneumatic sanding tool. The entire casting was sandblasted to remove any residual sand to prepare it for heat treatment. A piece of the gating was cut off to be used to test the hardness after heat treatment. Despite the high superheat during pouring the lattices on the sides did not completely fill, Figure 16. The core inserts that were pinned in-place shifted during pouring and caused a large void on one of the sides of the casting, Figure 16. In addition, there was significant flash inside the hammer and around the lettering inserts. In terms of surface finish, there were visible print lines on the sides of the casting, but the surface roughness was fairly good with most of the lettering was legible.

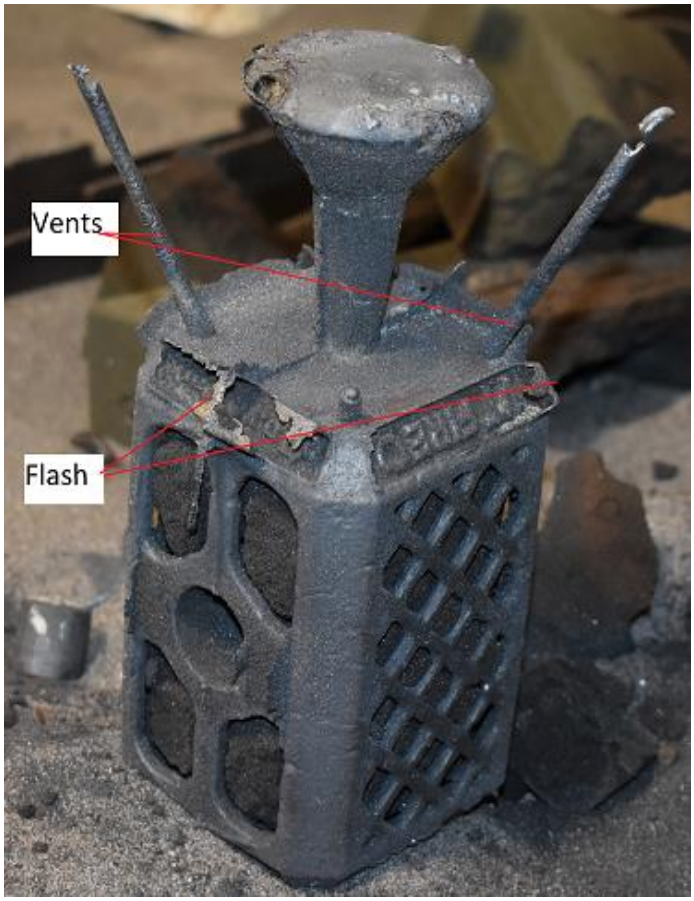

Figure 15. The casting after it was removed from the mold.

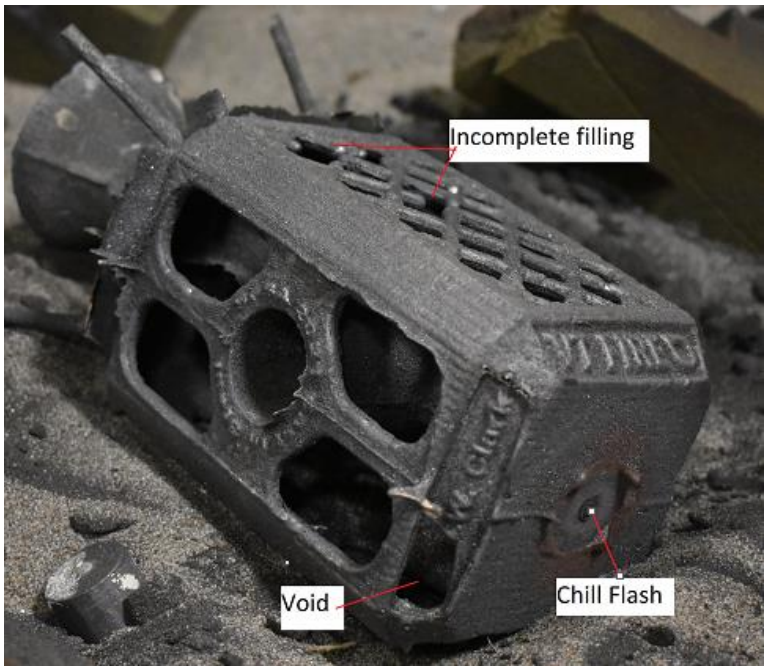

Figure 16. There was flash along the parting lines and a hole where the insert shifted.

Heat Treatment and Microscopy:

During solidification and cooling in the sand mold, the metal underwent the austenite to ferrite-pearlite transformation. The casting and a piece of the downspure were sent to Southwest Specialty Heat Treat for heat treatment. The first step of the heat treatment was to normalize the casting. Normalizing steel is a recrystallization heat treatment that is used to condition the casting before the final heat treatment [16]. It refines the structure and homogenizes the composition to produce more uniform mechanical properties [16] and more consistent heat treatment response. This process involves transforming the ferrite-pearlite to austenite by heating the material to the austenite range at 1,600^{o}F, which is then followed by slow cooling in air. This transforms the austenite into proeutectoid ferrite, pearlite plus (we believe) some martensite. We replicated this in our lab by heating a piece of the as-cast steel with a thermocouple embedded in it to the fully austenite range and then slowing cooling the piece in air. Figure 17 shows the time versus temperature behavior of the steel as it was heated and cooled as well as the transformation points. The transformation stop and start times were determined by plotting the change in temperature with time versus temperature. Figure 18 and Figure 19, in the appendix, show the plots of this data. With this, it was determined that upon heating the starting and ending temperatures to transform the ferrite-pearlite to austenite occurred at 1,126 and 1,266^{o}F. Upon cooling, the transformation start and stop times to turn the austenite into proeutectoid ferrite, pearlite occurred at 1,464 to 1,357^{o}F.

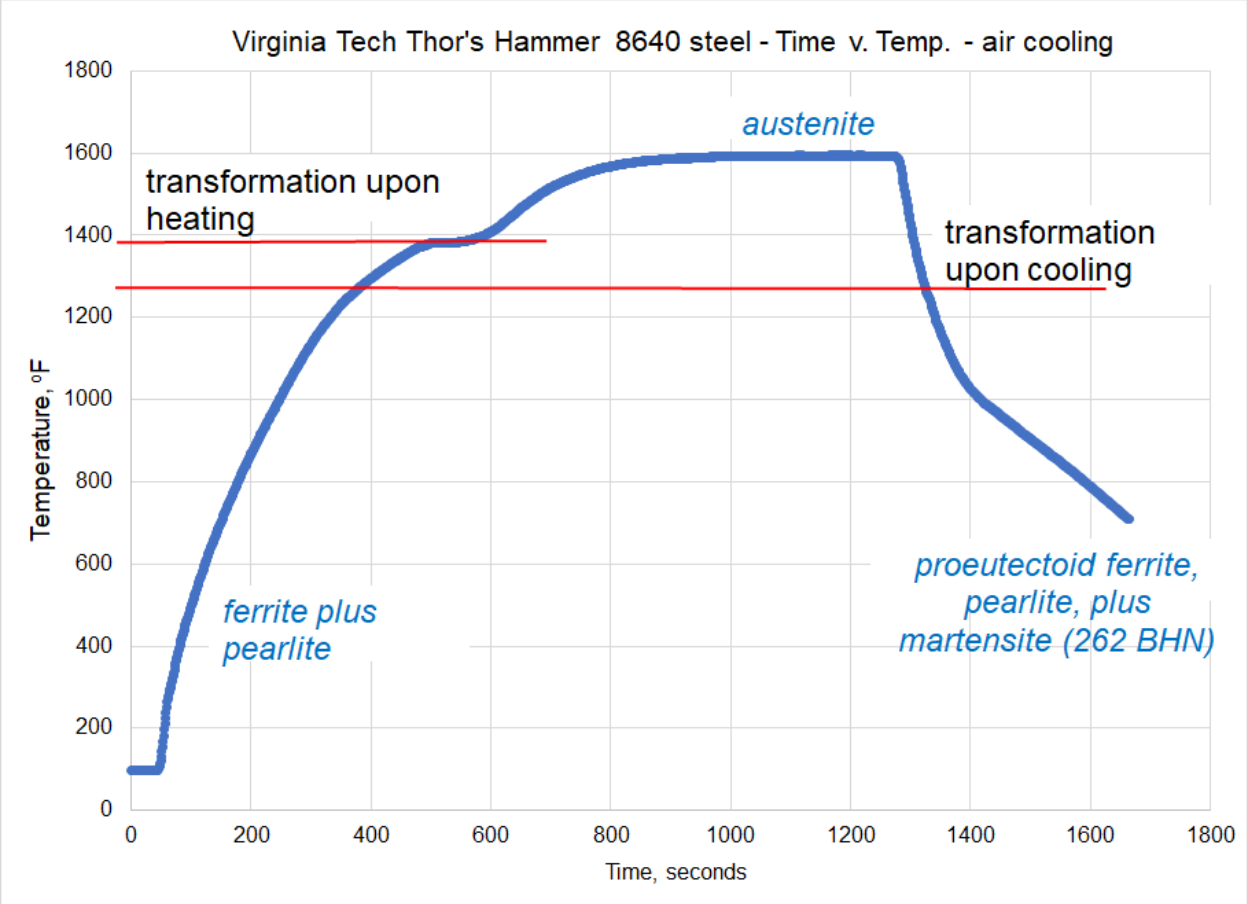

Figure 17. The graph shows the phase transformations upon heating and cooling.

After normalizing, the steel it was then again heated to the fully austenite range and then quenched in oil to transform the austenite into the hard martensitic phase. The casting was immediately tempered between 380 - 400°F for 1 hour followed by air cooling to room temperature. The tempering process transforms the untempered martensite into tempered martensite in order to increase ductility and toughness. The final Brinell hardness of the casting was 502 BHN (52 HRC). Brinell hardness was also taken on the as-cast piece and the air cooled (normalized) sample, Table 5.

Table 5. The Brinell values and their converted Rockwell C values.

As-Cast	Normalized	Quench & Tempered
255 BHN (26 HRC)	262 BHN (27 HRC)	502 BHN (52 HRC)

Microscopy samples were taken from the as-cast downsprue and the quenched and tempered test piece sent to Southwest specialty heat treaters. The samples were polished and etched with 4% Nital before imaging. Figure 20, shows that the as-cast

structure was dendritic with ferrite and pearlite. After quenching and tempering, the test piece was imaged at 100x, Figure 21, which shows the tempered martensite.

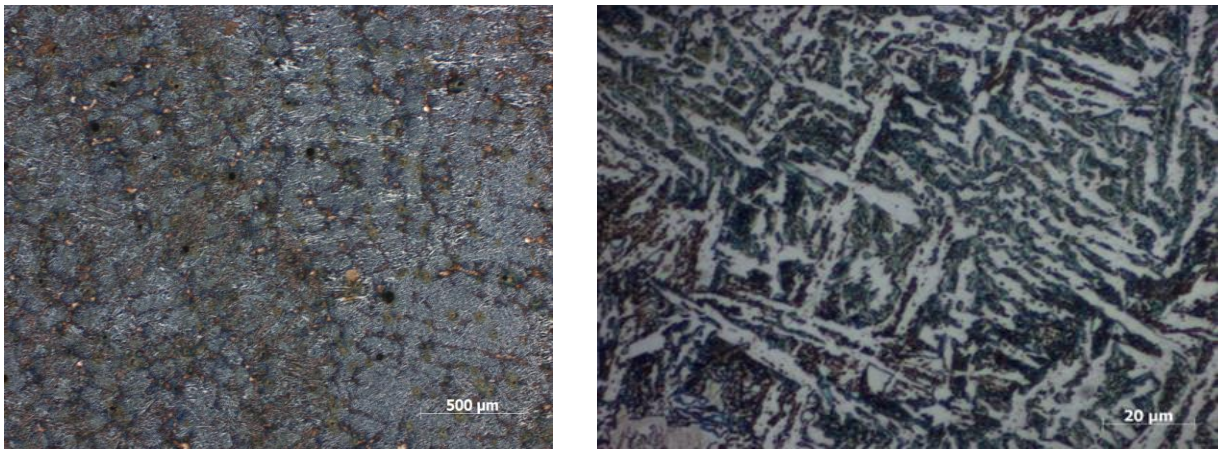

Figure 20. The dendritic structure at 50x (left) and the proeutectoid ferrite plus pearlite structure at 1000x (right) of the as-cast steel.

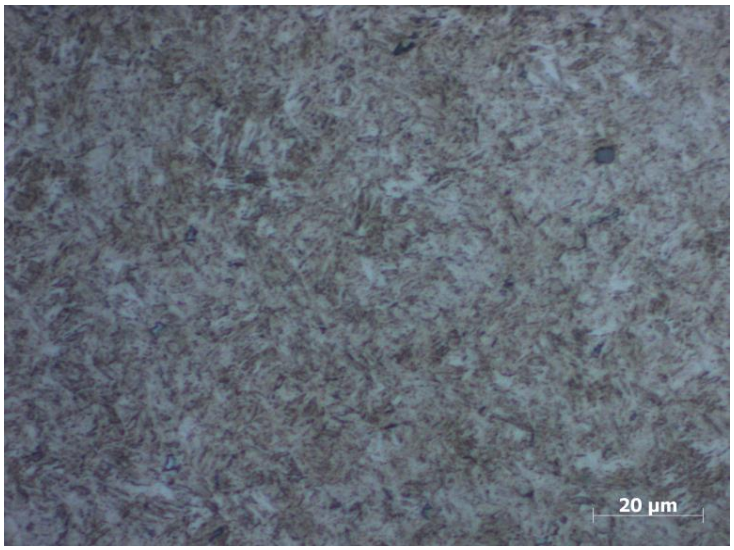

Figure 21. The microstructure of the quenched and tempered steel at 1000x showing tempered martensite.

Final Touches:

After heat treatment, the hammer head was grit blasted again to remove the oxide layer before it was sprayed with a lacquer to prevent rust. The weight of the hammer head was 5.2 lbs. An extruded fiberglass tube was used for the handle. The hole in the hammer head was widened using a pneumatic grinder to ensure the handle had a snug fit. The handle was affixed to the hammer head with West Systems G/flex, low modulus, epoxy resin that is specifically design for attaching scales to knives. This epoxy is resilient enough to bond dissimilar materials and flexible enough to absorb the stress of expansion, contraction, shock, and vibration. The inside of the hammer was

painted with a black lacquer to highlight the lattice work and details on the outside. The handle of the hammer was wrapped in a triple strand paracord design. The strap was added by drilling a hole at the end of the handle and tying more paracord. The ends were sealed and glued together with the same epoxy used to attach the handle. Figure 22 shows the finished hammer that was submitted for the competition. The final weight of the hammer with the handle was 5.7 lb. Dimensions of the hammer was 6” x 5” x 5” and a total of 16” tall. A replica prop of the Marvel Mjölnir is stated to be 17” tall and the hammerhead is 8” long and 5” wide, Figure 23 [17].

Figure 22. The hammer showing the painted details (left), and the full shot of the hammer (right).

Figure 23. The Marvel prop next to our finished hammer [17].

Current and Future Work:

Our industry partner (DW Clark) printed a second mold that they poured in 8630 (a common product for DW Clark). Table 6, lists their casting chemistry and the 8630 specification. We advised them to secure the lettering inserts and they were able to prevent them from slipping too much, Figure 24. They also had similar issues with filling the lattice on the sides of the casting. Unfortunately, due to time constraints, we were unable to get the foundry partner casting heat treated and finished in time for the competition. Our plan is to normalize, carburize the surface, quench and temper. This would produce a 60 HRC surface with a softer more ductile core. The finished hammer will be sent to D.W. Clark so they can put it on display.

Table 6. The D.W. Clark casting chemistry and 8630 steel specification [9].

Alloy	**C**	**Mn**	**P**	**S**	**Si**	**Ni**	**Cr**	**Mo**
D.W. Clark	0.32	0.78	0.020	0.004	0.62	0.46	0.53	0.21
8630	0.28-0.33	0.65-0.95	0.035 max	0.040 max	0.15-0.30	0.35-0.75	0.40-0.60	0.15-0.25

Figure 24. The lettering and cores did not shift, but the lattice still did not fill completely.

The main issues with our casting were incomplete fill of small cross section lattices and the inserts shifting during pouring. We are currently working with ExOne to reprint our mold by making the inner core one piece instead of a three part assembly. The second is to make the inserts part of the mold halves. Finally, we will increase the thickness of the lattice on the side. We plan on casting this in 8640 steel again and putting it on display in the Materials Science and Engineering Department at Virginia Tech.

Citations:

[1] J. Lindow and J. Lindow, *Norse Mythology: A Guide to Gods, Heroes, Rituals, and Beliefs*. Cary, UNITED STATES: Oxford University Press USA - OSO, 2002.

[2] J. Zhang, “Viking-Era Jewelry: Revealing an Intricate Cultural History of the Ancient Norsemen.”

[3] A. Scarsi, “‘Thor’s Hammer’ discovered in Iceland - shock Viking find,” *Express.co.uk*, Oct. 19, 2018.

[4] “Mjølnir,” *Marvel Cinematic Universe Wiki*. https://marvelcinematicuniverse.fandom.com/wiki/Mj%C3%B8lnir.

[5] “3d rendering of thor hammer near engineering drawing,” *iStock*.

[6] G. Johnson and W. H. Cook, “A constitutive model and data for materials subjected to large strains, high strain rates, and high temperatures,” in *Proceedings : Seventh International Symposium on Ballistics*, 1983, pp. 541–547, [Online].

[7] J. O. Hallquist, *LS-DYNA Keyword user’s manual*, vol. II. Livermore, CA, 2020.

[8] MAGMASOFT®. (1989-2018). Magma GmbH, Aachen, Germany. [Online]. Available; https://www.magmasoft.com/en/

[9] D. Poweleit, “Steel Castings Properties,” in *Casting*, vol. 15, S. Viswanathan, D. Apelian, R. J. Donahue, B. DasGupta, M. Gywn, J. L. Jorstad, R. W. Monroe, M. Sahoo, T. E. Prucha, and D. Twarog, Eds. ASM International, 2008, pp. 949–974.

[10] J. L. Dossett and G. E. Totten, Eds., “Steel Selection for Hardening,” in *Heat Treating of Irons and Steels*, ASM International, 2014, pp. 29–43.

[11] “Striking Tools,” *Urrea Professional Tools*.

[12] J. O. Andersson, T. Helander, L. Höglund, P. F. Shi, and B. Sundman, *Thermo-Calc and DICTRA, Computational tools for materials science*. .

[13] I. Gibson, D. Rosen, B. Stucker, and M. Khorasani, “Binder Jetting,” in *Additive Manufacturing Technologies*, I. Gibson, D. Rosen, B. Stucker, and M. Khorasani, Eds. Cham: Springer International Publishing, 2021, pp. 237–252.

[14] “ExOne’s Family of Sand 3D Printers.” https://www.exone.com/en-US/3D-printing-systems/sand-3d-printers.

[15] “Foundry Robotic 3D Printers Archives,” *EnvisionTEC*. https://envisiontec.com/3d-printers/robotic-additive-manufacturing/.

[16] J. L. Dossett and G. E. Totten, Eds., “Heat Treating of Low-Alloy Steels,” in *Heat Treating of Irons and Steels*, vol. 4D, ASM International, 2014, pp. 122–168.

[17] “Marvel Thor Hammer Prop Replica by Museum Replicas,” *Sideshow Collectibles*. https://www.sideshow.com/collectibles/marvel-thor-hammer-museum-replicas-901440.

Appendix:

				Steel Charge Calulations						
	Material	C	Si	Mn	Ni	Cu	Mo	Fe	Cr	
	sorel	4.2	0.07	0.008	0	0	0	95.722	0	
	liquid before alloying	0.055	0.014	0.055	0.008	0.042	0.007	99.79	0.029	
	FeMo	0.08	1.44				65.03	33.45		
	Ni	0			100					
	FeMn	6.5		79.5	0			14		
	75FeSi		75			0		25		
	Cr						0	0	99.5	
				Sept. 10, 2019						
Lbs of	Material	C	Si	Mn	Ni	Cu	Mo	Fe	Cr	
8.46	sorel	0.35532	0.005922	0.0006768	0	0	0	8.098081	0	
100	liquid before alloying	0.055	0.014	0.055	0.008	0.042	0.007	99.790	0.029	
0.33	FeMo	0.000264	0	0	0	0	0.214599	0.110385	0	
0.72	Ni	0	0	0	0.72	0	0	0	0	
1.2	FeMn	0.078	0	0.954	0	0	0	0.168	0	
0.57	75FeSi	0	0.4275	0	0	0	0	0.1425	0	
0.59	Cr	0	0	0	0	0	0	0	0.58705	
111.87	total	0.489	0.447	1.010	0.728	0.042	0.222	108.309	0.616	lbs
		0.44%	0.40%	0.90%	0.65%	0.038%	0.20%	96.82%	0.55%	wt%
	target: 8640	0.35-0.45	0.20-0.80	0.70-1.05	0.40-0.70		0.15 - 0.25		0.40-0.60	
	actual									
	aluminum shot in ladle:	0.0045	lbs							
		2.0412	grams							

Figure 14. The charge calculations for the 8640 alloy with the amount of aluminum shot added to kill the steel in the ladle.

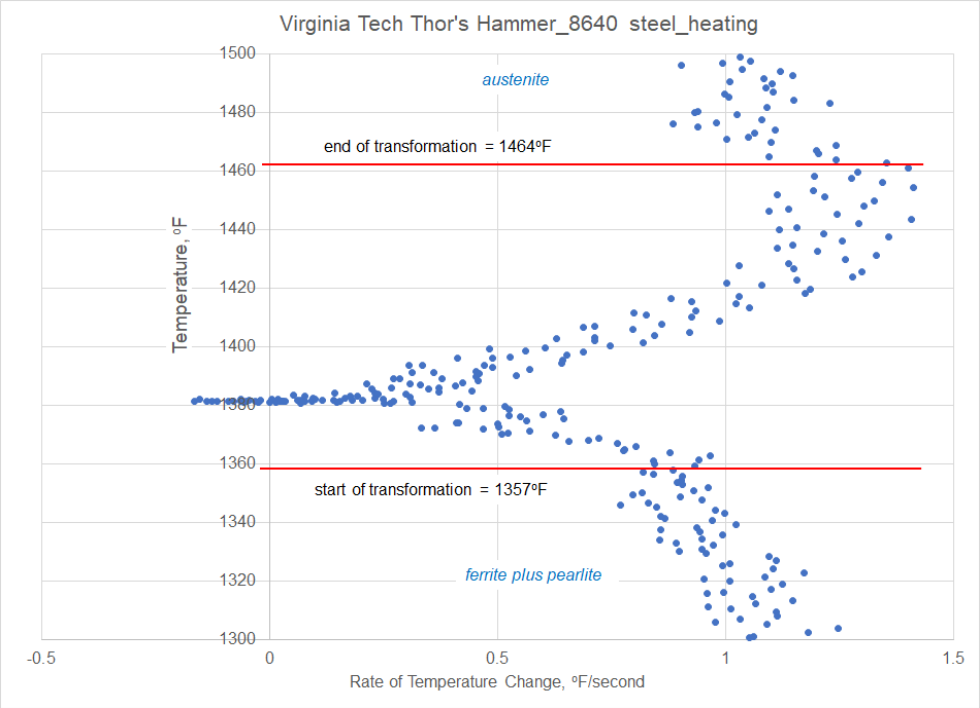

Figure 18. The rate of temperature change shows the transformation start and stop temperatures upon heating.

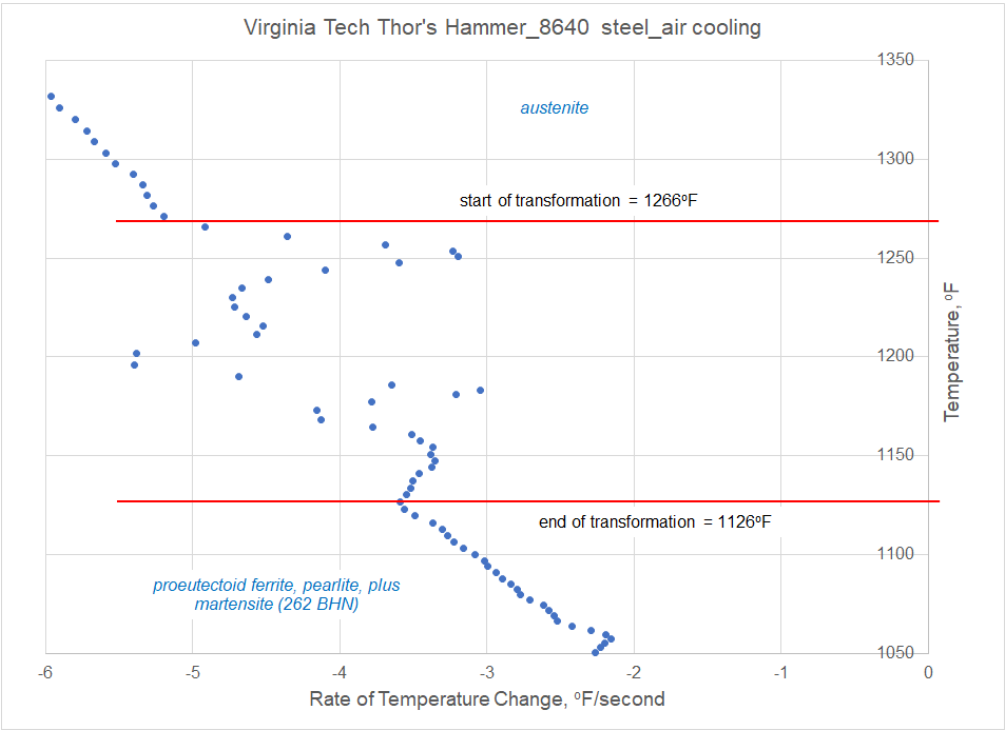

Figure 19. The rate of temperature change shows the transformation start and stop temperatures upon cooling.